



**HAL**  
open science

# The Chain Manganates $K_{29}Mn_{17}O_{34}$ , $Rb_{11}Mn_8O_{16}$ and $Cs_4Mn_3O_6$ : a New Family of Mixed-valent One-dimensional Transition Metallates

Steffen Pfeiffer, Jürgen Nuss

► **To cite this version:**

Steffen Pfeiffer, Jürgen Nuss. The Chain Manganates  $K_{29}Mn_{17}O_{34}$ ,  $Rb_{11}Mn_8O_{16}$  and  $Cs_4Mn_3O_6$ : a New Family of Mixed-valent One-dimensional Transition Metallates. *Journal of Inorganic and General Chemistry / Zeitschrift für anorganische und allgemeine Chemie*, 2009, 636 (1), pp.23. 10.1002/zaac.200900269 . hal-00507772

**HAL Id: hal-00507772**

**<https://hal.science/hal-00507772>**

Submitted on 31 Jul 2010

**HAL** is a multi-disciplinary open access archive for the deposit and dissemination of scientific research documents, whether they are published or not. The documents may come from teaching and research institutions in France or abroad, or from public or private research centers.

L'archive ouverte pluridisciplinaire **HAL**, est destinée au dépôt et à la diffusion de documents scientifiques de niveau recherche, publiés ou non, émanant des établissements d'enseignement et de recherche français ou étrangers, des laboratoires publics ou privés.



**The Chain Manganates  $K_{29}Mn_{17}O_{34}$ ,  $Rb_{11}Mn_8O_{16}$  and  $Cs_4Mn_3O_6$ : a New Family of Mixed-valent One-dimensional Transition Metallates**

Journal:	<i>Zeitschrift für Anorganische und Allgemeine Chemie</i>
Manuscript ID:	zaac.200900269
Wiley - Manuscript type:	Article
Date Submitted by the Author:	12-May-2009
Complete List of Authors:	Pfeiffer, Steffen; Max-Planck-Institute for Solid State Research, Chemistry III Nuss, Jürgen; Max-Planck-Institute for Solid State Research, Chemistry III
Keywords:	Azide/nitrate route, Chain structures, Magnetic properties, Manganese, Mixed-valent compounds



## ARTICLE

DOI: 10.1002/zaac.200((will be filled in by the editorial staff))

# The Chain Manganates $K_{29}Mn_{17}O_{34}$ , $Rb_{11}Mn_8O_{16}$ and $Cs_4Mn_3O_6$ : a New Family of Mixed-valent One-dimensional Transition Metallates

Steffen Pfeiffer,<sup>[a]</sup> Jürgen Nuss,<sup>[a]</sup> and Martin Jansen\*<sup>[a]</sup>

*Dedicated to Professor Arndt Simon on the Occasion of His 70th Birthday*

**Keywords:** Azide/nitrate route; Chain structures; Magnetic properties; Manganese; Mixed-valent compounds

**Abstract.** Air and moisture sensitive  $K_{29}Mn_{17}O_{34}$ ,  $Rb_{11}Mn_8O_{16}$  and  $Cs_4Mn_3O_6$  have been prepared via the azide/nitrate route from stoichiometric mixtures of the precursors  $Mn_2O_3$ ,  $AN_3$  and  $ANO_3$  ( $A = K, Rb, Cs$ ) in special containers provided with silver inlays. Their compositions can be generalized as  $A_xMnO_2$  with  $x$  varying between 1.703 and 1.333. According to the X-ray analysis of the crystal structures [ $K_{29}Mn_{17}O_{34}$ : *Ima2*,  $Z = 4$ ,  $a = 93.149(3)$ ,  $b = 10.0063(3)$ ,  $c = 6.0621(2)$  Å, 6585 independent reflections,  $R_1 = 0.053$ ,  $wR(\text{all}) = 0.143$ ;  $Rb_{11}Mn_8O_{16}$ : *F222*,  $Z = 16$ ,  $a = 12.2096(4)$ ,  $b = 20.1595(7)$ ,  $c = 43.712(2)$  Å, 11534 independent reflections,  $R_1 = 0.042$ ,  $wR(\text{all}) = 0.131$ ;  $Cs_4Mn_3O_6$ : *C222*,  $Z = 8$ ,  $a = 12.790(3)$ ,  $b = 21.123(4)$ ,  $c = 8.179(2)$  Å, 2212 independent reflections,  $R_1 =$

0.051,  $wR(\text{all}) = 0.122$ ], the main feature of all three crystal structures are  ${}^1_{\infty}MnO_2^{n-}$  chains built up from partially distorted edge-sharing  $MnO_4$  tetrahedra. The alkali metal ions fill the space between the anionic entities forming honeycomb like arrangements.

In all cases manganese is in a mixed-valent state but no full charge ordering is noticeable. The variations of the charges along the  $MnO_2^{n-}$  chains seem to be best described in terms of charge density waves. The magnetic susceptibilities show the dominance of strong antiferromagnetic interactions for the rubidium and the cesium compounds, whereas ferro- or ferrimagnetic interactions prevail in the potassium compound.

\* Prof. Dr. M. Jansen  
Fax: +49-711-689-1502  
E-Mail: M.Jansen@fkf.mpg.de  
[a] Max-Planck-Institut für Festkörperforschung  
Heisenbergstr. 1  
D-70569 Stuttgart, Germany

of competing magnetic exchange interactions [5, 6], while  $Na_3Cu_2O_4$  and  $Na_8Cu_5O_{10}$  show a specific charge ordering pattern that qualify them as the first unambiguous manifestations of a Wigner crystal [7, 8].

Manganese stands out from the other transition elements because of its richness in accessible oxidation states, and thus appears to be a well suited candidate for further probing the potential of the azide/nitrate route. Since most of the transition metal oxides with low dimensional partial structures have the general composition  $A_xTO_2$  we have focused our efforts on oxomanganates  $A_xMnO_2$ . Thus far, respective mixed-valent representatives have only been identified for the combination  $Mn^{3+}/Mn^{4+}$ . Among them are the Hollandites (e.g.  $Ba_{1-x}Mn_4O_8$  [9],  $Rb_{1-x}Mn_4O_8$  [10] or  $Ag_{1-x}Mn_4O_8$  [11],  $0 \leq x \leq 0.24$ ) and spinel derivatives like  $LiMn_2O_4$  [12]. With the exception of  $CsMnO_2$ , all members of the family  $AMnO_2$  ( $A = Li, Na, K, Rb$ ) are known and have been characterized, at least structurally [13-18]. For divalent manganese, in addition to the mixed alkali manganates(II)  $Li_5Na_3Mn_5O_9$ ,  $LiKMnO_2$ ,  $LiRbMn_3O_4$  and  $NaKMnO_2$  [19-22],  $Na_2MnO_2$  was reported recently [23]. Although the binary manganese (II, III) oxide  $Mn_3O_4$ , occurring naturally as the mineral Hausmannite, is known to be pretty stable, hardly any ternary manganese (II/III) mixed-valent compounds are known. Lithium intercalated  $Mn_3O_4$ ,  $LiMn_3O_4$  [24], and  $Na_{26}Mn_{39}O_{55}$  [25] are the only representatives reported so far. The prominent feature of the latter is a  $T5$  supertetrahedron consisting of 35 interlinked  $MnO_4$  tetrahedra.

By increasing the alkali metal to manganese ratio beyond the values typical for hollandites, we have been able to shift

## Introduction

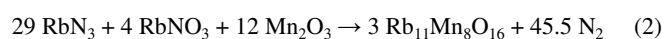
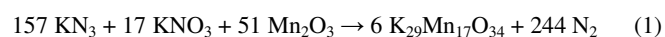
Oxides continue to be a central field of activities in solid state and materials research. A lot of motivation originates from conspicuous properties like high  $T_c$  superconductivity or extreme magnetoresistance as discovered to occur in some multinary transition metal oxides [1, 2]. Although a detailed microscopic understanding of the underlying mechanisms is still lacking, the bulk properties appear to be associated with the phenomena of charge, spin and orbital ordering in solids displaying low dimensional substructures. During our studies on alkali oxometallates, employing the azide/nitrate route [3, 4], we became aware that as compared to reacting the binary constituting oxides this synthetic approach is featuring several highly beneficial characteristics, like significantly increased free enthalpy of reaction and improved kinetic activation. More importantly, the total composition of the respective product, in particular its oxygen content and thus the valence state of the transition metal involved, can be well controlled by weighing in the alkali metal azides and nitrates in an appropriate ratio. This is reflected by a number of interesting mixed valent ternary transition metallates with intriguingly complex compositions synthesized along this route. For example,  $Na_{10}Co_4O_{10}$  shows four different types

the oxidation state of manganese to lower values (2+/3+) and to break down the three-dimensional framework of the anionic MnO<sub>2</sub> part of the Hollandite to a one-dimensional partial structure. The compositions realized, K<sub>29</sub>Mn<sub>17</sub>O<sub>34</sub>, Rb<sub>11</sub>Mn<sub>8</sub>O<sub>16</sub> and Cs<sub>4</sub>Mn<sub>3</sub>O<sub>6</sub> can be generalized as A<sub>x</sub>MnO<sub>2</sub> with *x* varying between 1.706 and 1.333, reflecting the structurally similar one-dimensional oxometallate anion present in all three representatives.

## Experimental Section

### Synthesis

Starting materials for the preparation of the title compounds were Mn<sub>2</sub>O<sub>3</sub> (99.9%, Chempur, Karlsruhe, Germany), KNO<sub>3</sub> (99.5%, Riedel-de Haën, Seelze, Germany), RbNO<sub>3</sub> (99%, Johnson Matthey, Sulzbach, Germany) and CsNO<sub>3</sub> (99.9%, Acros Organics, Geel, Belgium). The respective azides were synthesized from aqueous HN<sub>3</sub> and potassium carbonate (99%, Sigma-Aldrich, Steinheim, Germany), rubidium carbonate (99%, Johnson Matthey) and cesium carbonate (99%, Sigma-Aldrich) [26]. The starting materials were mixed in the ratio required according to the general Equations (1-3):



The mixtures were ground thoroughly in an agate mortar and pressed to pellets under 10<sup>5</sup> N, dried in vacuum (10<sup>-3</sup> mbar) at 400 K for 12 h, and placed under argon in a tightly closed steel container, provided with a silver inlay [3, 4]. In a flow of dried argon the following temperature profile was applied for the potassium compound: 298 → 533 K (100 K/h), 533 → 673 K (5 K/h), 673 → 873 K (20 K/h), and subsequent annealing for 100 h at 873 K. The temperature profile for the two other compounds was slightly different: 298 → 533 K (100 K/h), 533 → 653 K (5 K/h), 653 → 773 K (20 K/h), and subsequent annealing for 30 h at 773 K.

**Hazards:** *If heated too rapidly the containers may blow up!*

The obtained black powders are very sensitive to humid air, and were therefore sealed in glass ampoules under argon atmosphere and all following manipulations with these substances were performed in inert atmospheres of purified argon.

Single crystals of K<sub>29</sub>Mn<sub>17</sub>O<sub>34</sub>, Rb<sub>11</sub>Mn<sub>8</sub>O<sub>16</sub> and Cs<sub>4</sub>Mn<sub>3</sub>O<sub>6</sub> have been grown by subsequent annealing of the reaction products, however, applying an excess of potassium-, rubidium- and cesium-oxide of (K<sub>2</sub>O, Rb<sub>2</sub>O, Cs<sub>2</sub>O) : MnO = 2 : 1, respectively, for 100 h at 873 K for K<sub>29</sub>Mn<sub>17</sub>O<sub>34</sub> and 500 h at 723 K for the rubidium and cesium compounds. For this purpose, the micro-crystalline primary product was pressed in a pellet and placed in a silver crucible, closed with a silver stopper, which was then sealed in a glass ampoule under dried argon.

### X-ray Diffraction

X-ray investigations on powder samples were performed using a STOE StadiP diffractometer (Stoe & Cie, Darmstadt, Germany)

supplied with a position sensitive detector (external reference: Si, *a* = 5.43088(4) Å) and a curved germanium monochromator with MoKα<sub>1</sub> radiation (λ = 0.70930 Å) at room temperature. Data were collected in the range of 3 to 40° in 2θ.

Crystals for single crystal diffraction were mounted in glass capillaries inside a dry-box (M. Braun, Garching, Germany). Data were collected on a three-circle diffractometer, equipped with an APEX I CCD detector (Bruker AXS, Karlsruhe, Germany), at room temperature. The intensities were integrated with the *SAINTE* program in the *Bruker Suite* software package [27], and semi-empirical absorption correction (*SADABS* [28]) was applied. All three representatives crystallize in acentric space groups: *Ima2* (K<sub>29</sub>Mn<sub>17</sub>O<sub>34</sub>), *F222* (Rb<sub>11</sub>Mn<sub>8</sub>O<sub>16</sub>) and *C222* (Cs<sub>4</sub>Mn<sub>3</sub>O<sub>6</sub>). The structures were solved by direct methods and refined by full-matrix least squares using *SHELXTL* program package [29]. It was not possible to determine the absolute structure during the structure refinements; racemic twinning was assumed in each case, which slightly improved the *R*-values. Experimental details are given in Table 1, atom coordinates and equivalent isotropic displacement parameters in Tables 2-4. All atoms were treated with anisotropic displacement parameters except for O7 in Cs<sub>4</sub>Mn<sub>3</sub>O<sub>6</sub>, which was described best with a split position and isotropic temperature parameters [30].

### Thermal Analysis

Thermal analyses were carried out using a DTA/TG device (STA 409, Netzsch, Selb, Germany) coupled with a quadrupole mass spectrometer (QMG 421, Balzers, Lichtenstein). The samples were heated at a rate of 10 K min<sup>-1</sup> in corundum crucibles, under dried argon.

### Magnetic Measurements

Magnetic susceptibilities were measured in the temperature ranges from 5 to 300 K (K<sub>29</sub>Mn<sub>17</sub>O<sub>34</sub>), 2 to 550 K (Rb<sub>11</sub>Mn<sub>8</sub>O<sub>16</sub>) and 2 to 450 K (Cs<sub>4</sub>Mn<sub>3</sub>O<sub>6</sub>), in magnetic fields from 0.001 to 1 T (K<sub>29</sub>Mn<sub>17</sub>O<sub>34</sub>) and from 0.001 to 5 T (Rb<sub>11</sub>Mn<sub>8</sub>O<sub>16</sub>, Cs<sub>4</sub>Mn<sub>3</sub>O<sub>6</sub>) using a SQUID-Magnetometer (MPMS 5.5, Quantum Design, San Diego, USA).

## Results and Discussion

The title compounds K<sub>29</sub>Mn<sub>17</sub>O<sub>34</sub>, Rb<sub>11</sub>Mn<sub>8</sub>O<sub>16</sub> and Cs<sub>4</sub>Mn<sub>3</sub>O<sub>6</sub> have been prepared along the azide/nitrate route [3, 4] as black, microcrystalline, pure phases in gram amounts. They start to decompose at about 910 K (K<sub>29</sub>Mn<sub>17</sub>O<sub>34</sub>) and 940 K (Rb<sub>11</sub>Mn<sub>8</sub>O<sub>16</sub>, Cs<sub>4</sub>Mn<sub>3</sub>O<sub>6</sub>).

The new oxomanganates(II/III) belong to the compositional series A<sub>x</sub>MnO<sub>2</sub> (A = K, Rb, Cs), with end members AMnO<sub>2</sub> [13-18] and for K, Rb, and Cs still elusive A<sub>2</sub>MnO<sub>2</sub>. The most prominent structural feature, shared by all three compounds, is a one-dimensional polyanion <sup>1</sup><sub>∞</sub>MnO<sub>2</sub><sup>n-</sup> constituted of edge sharing sometimes heavily distorted MnO<sub>4</sub> tetrahedra, see Figure 1.

In the case of K<sub>29</sub>Mn<sub>17</sub>O<sub>34</sub>, the <sup>1</sup><sub>∞</sub>MnO<sub>2</sub><sup>n-</sup> chains, running along the *a*-axis, are slightly undulating with an amplitude of approximate 0.5 Å and ∠<sub>Mn-Mn-Mn</sub> angles ranging between 161 and 177°, whereby the oxygen tetrahedra are in a

staggered conformation, as one would expect for chains of trans-edge sharing tetrahedra. The potassium ions achieve coordination numbers ranging from 4 to 6, and the bond lengths  $d(\text{K—O})$  are in the plausible range, reaching from 2.55 to 3.35 Å. The  ${}^1_{\infty}\text{MnO}_2^{n-}$  chains in  $\text{Rb}_{11}\text{Mn}_8\text{O}_{16}$  and  $\text{Cs}_4\text{Mn}_3\text{O}_6$  are running along the  $c$ -axis and the  $\angle_{\text{Mn—Mn—Mn}}$  angles amount to exactly  $180^\circ$  because all Mn atoms are located on special positions, for both representatives (see Table 3 and 4). The oxygen atoms are screwed along Mn-backbone, in order to avoid short alkali-metal—oxygen distances which are in the expected range from 2.70–3.63 Å and 2.88–3.73 Å, respectively. The coordination numbers around the alkali metal ions vary between 5 and 8. The  ${}^1_{\infty}\text{MnO}_2^{n-}$  screws are particularly well visible in  $\text{Rb}_{11}\text{Mn}_8\text{O}_{16}$  (Figure 1b and 2b). The respective helix in  $\text{Cs}_4\text{Mn}_3\text{O}_6$  is perturbed because of the split position of O7. This results in two possible orientations for the  $\text{Mn}_7\text{O}_6\text{O}_7$  tetrahedra (pink colored tetrahedra in Figure 1c and 2c). In all three compounds the alkali metal ions fill the space between the anionic entities forming honeycomb like arrangements. The projection of the crystal structures along the longest axis (in each case the direction along which the  $\text{MnO}_2^{n-}$  chains extend) is displayed in Figure 2.

From the compositions it is obvious that in each case manganese is in a mixed-valent state. One could assign average or split valences according to  $\text{K}_{29}\text{Mn}^{\text{II}}_{12}\text{Mn}^{\text{III}}_{5}\text{O}_{34}$  (+2.294),  $\text{Rb}_{11}\text{Mn}^{\text{II}}_3\text{Mn}^{\text{III}}_5\text{O}_{16}$  (+2.625) and  $\text{Cs}_4\text{Mn}^{\text{II}}\text{Mn}^{\text{III}}_2\text{O}_4$  (+2.667). Fully ordered charges should be reflected by specific Mn—O distances. For a tetrahedral coordination one would expect Mn—O bond lengths of 1.9 Å ( $\text{Mn}^{3+}$ ) and 2.0 Å ( $\text{Mn}^{2+}$ ), respectively. These approximate distances are derived from known structures, like  $\text{A}_6\text{Mn}_2\text{O}_6$  ( $A = \text{K}, \text{Rb}$ ) [32] or  $\text{Na}_2\text{MnO}_2$  [23]. At inspecting Table 5, where the interatomic distances between manganese and oxygen are given, one notices significant spreads from 1.84 to 2.06 Å, well covering the full range as expected for  $\text{Mn}^{3+}$  and  $\text{Mn}^{2+}$  distances to oxygen. However, attempts to consistently assign charges to specific manganese atoms have failed because of discrepancies arising between the Wyckhoff multiplicities and the ratio of  $\text{Mn}^{2+}/\text{Mn}^{3+}$  required for electroneutrality. This is demonstrated at the example of  $\text{Rb}_{11}\text{Mn}^{\text{II}}_3\text{Mn}^{\text{III}}_5\text{O}_{16}$ . For  $Z = 16$  there are 128 manganese atoms in the unit cell, distributed over 17 independent crystallographic sites. Mn1 and Mn2 are occupying a four fold site, while all other manganese ions are occupying eight fold sites. 48  $\text{Mn}^{2+}$  are needed to warrant charge neutrality. This can be achieved by occupying six eight fold sites or by occupying five eight fold sites and the two four fold sites. However, according to Table 5 the Mn1—O distance is the shortest one in the crystal structure while the Mn2—O distance is one of the longest in the whole structure. Thus it is impossible to generate the required  $\text{Mn}^{2+}/\text{Mn}^{3+}$  ratio with neither of the occupancies possible. What was shown explicitly for  $\text{Rb}_{11}\text{Mn}_8\text{O}_{16}$  holds true for the other two compounds as well.

The magnetic susceptibilities of  $\text{K}_{29}\text{Mn}_{17}\text{O}_{34}$ ,  $\text{Rb}_{11}\text{Mn}_8\text{O}_{16}$  and  $\text{Cs}_4\text{Mn}_3\text{O}_6$  have been measured in magnetic fields ranging from 0.001 to 5 T. Only in the case of the potassium compound the susceptibility showed a dependency on the field strength. To enable comparison of the magnetic behavior of all three compounds the susceptibilities at 1 T and per one manganese atom are shown in Figure 3. In each case the magnetic response of the unpaired spins present appears to be considerably quenched by magnetic exchange

interactions, and within the temperature range considered, no transition to a paramagnetic regime was observed. Since the super exchange coupling along Mn—O—Mn bridges is assumed to be weak due to the angle at oxygen approaching  $90^\circ$ , direct Mn—Mn interactions mediated by  $d_z^2$  orbitals need to be involved. Qualitatively, the rubidium and cesium compounds show a rather similar behavior, while the trace of the susceptibility of the potassium compound is qualitatively different. This might be attributed to the larger amount of divalent manganese atoms in the latter compound. Since the  $\text{Mn}^{3+}$ —O separation is shorter than the  $\text{Mn}^{2+}$ —O distance the overlap of the Mn  $d_z^2$  orbitals in  $\text{K}_{29}\text{Mn}_{17}\text{O}_{34}$  is expected to be smaller than in the rubidium or cesium compounds. A larger overlap would lead to stronger antiferromagnetic interactions. Since  $\text{Rb}_{11}\text{Mn}_8\text{O}_{16}$  and  $\text{Cs}_4\text{Mn}_3\text{O}_6$  contain more  $\text{Mn}^{3+}$  than  $\text{K}_{29}\text{Mn}_{17}\text{O}_{34}$  the antiferromagnetic exchange interactions in the two former compounds should be much stronger. In order to derive a convincing model, experimental input from neutron diffraction is indispensable, respective experiments are currently under preparation.

## Conclusions

The manganates  $\text{K}_{29}\text{Mn}_{17}\text{O}_{34}$ ,  $\text{Rb}_{11}\text{Mn}_8\text{O}_{16}$  and  $\text{Cs}_4\text{Mn}_3\text{O}_6$  represent a new family of mixed-valent one-dimensional transition metallates containing  ${}^1_{\infty}\text{MnO}_2^{n-}$  chains running along one of the respective crystallographic axis which is rather long in the case of the K- and Rb-compound (Table 1). The exceptional lattice dimensions are caused by the need to adjust the translation period of  $\text{MnO}_2$  chains to the alkali metal frameworks. For  $\text{Cs}_4\text{Mn}_3\text{O}_6$  a simple formula for the average compatible periodicities can be given:  $3 \times d(\text{Mn—Mn}) = 2 \times d(\text{Cs—Cs}) = c$ . Finding the smallest common denominator in  $\text{K}_{29}\text{Mn}_{17}\text{O}_{34}$  leads to  $34 \times d(\text{Mn—Mn}) = 29 \times d(\text{K—K}) = a$  and  $16 \times d(\text{Mn—Mn}) = 11 \times d(\text{Rb—Rb}) = c$  for  $\text{Rb}_{11}\text{Mn}_8\text{O}_{16}$ . By complying the translation vectors of the  ${}^1_{\infty}\text{MnO}_2^{n-}$  polyanions and the respective alkali ions the oxidation state of manganese is fixed. The smaller cation generates a larger ratio between alkali metal and manganese in  $\text{K}_{29}\text{Mn}_{17}\text{O}_{34} = \text{K}_{1.706}\text{MnO}_2$  and consequently a larger ratio of  $\text{Mn}^{2+}/\text{Mn}^{3+} = 0.71/0.29$ . The bigger cesium ion requires a smaller ratio  $\text{Cs}/\text{Mn}$  ( $\text{Cs}_4\text{Mn}_3\text{O}_6 = \text{Cs}_{1.333}\text{MnO}_2$ ) and thus a smaller ratio  $\text{Mn}^{2+}/\text{Mn}^{3+} = 0.33/0.67$ . The rubidium compound lies in-between ( $\text{Rb}_{1.375}\text{MnO}_2$ ).

The variations of the charges of manganese along the  $\text{MnO}_2^{n-}$  chains seem to be more appropriately addressed in terms of charge density waves instead of a sequence of integral charges localized at the manganese sites. In particular, if one includes incommensurate contributions, access to such a physically more appropriate description could be opened. Indeed, some unusually large temperature parameters of individual alkali metal and oxygen ions, the split-position of one oxygen atom in  $\text{Cs}_4\text{Mn}_3\text{O}_6$ , and the racemic twinning are indicating a still not fully convincing crystallographic description, and an in depth investigation applying tools of higher dimensional crystallography appears desirable. This will be published elsewhere for  $\text{Rb}_{11}\text{Mn}_8\text{O}_{16}$  [33].

## Acknowledgments

The authors gratefully acknowledge Mrs. E. Brücher for magnetic measurements, and Dr. C. P. M. Oberndorfer for DTA/TG measurements.

## References

- [1] R. J. Cava, *Chem Comm.* **2005**, 43, 5373.
- [2] W. P. Pratt, S. F. Lee, J. M. Slaughter, R. Looee, P. A. Schroeder, J. Bass, *Phys. Rev. Lett.* **1991**, 66, 3060.
- [3] D. Trinschek, M. Jansen, *Angew. Chem.* **1999**, 111, 234. *Angew. Chem. Int. Ed. Engl.* **1999**, 38, 133.
- [4] M. Sofin, E. M. Peters, M. Jansen, *Z. Anorg. Allg. Chem.* **2002**, 628, 2697.
- [5] M. Sofin, H.-U. Güdel, R. Bircher, E. M. Peters, M. Jansen, *Angew. Chem.* **2003**, 115, 3651, *Angew. Chem. Int. Ed. Engl.* **2003**, 42, 3527.
- [6] N. Stüßer, M. Sofin, R. Bircher, H.-U. Güdel, M. Jansen, *Chem. Eur. J.* **2006**, 12, 5452.
- [7] M. Sofin, E. M. Peters, M. Jansen, *J. Solid State Chem.* **2005**, 178, 3708.
- [8] P. Horsch, M. Sofin, M. Mayr, M. Jansen, *Phys. Rev. Lett.* **2005**, 94, 76403.
- [9] H. Miura, *Mineral. J.* **1986**, 13, 119.
- [10] N. Yamamoto, Y. Oka, O. Tamada, *Mineral. J.* **1990**, 15, 41.
- [11] F. M. Chang, M. Jansen, *Angew. Chem.* **1984**, 96, 902, *Angew. Chem. Int. Ed. Engl.* **1984**, 23, 906.
- [12] A. Mosbah, A. Verbaere, M. Tournoux, *Mater. Res. Bull.* **1983**, 18, 1375.
- [13] G. Ditrach, R. Hoppe, *Z. Anorg. Allg. Chem.* **1969**, 368, 262.
- [14] J. P. Parant, R. Olazcuaga, M. Devalette, C. Fouassier, P. Hagenmuller, *J. Solid State Chem.* **1971**, 3, 1.
- [15] M. Jansen, R. Hoppe, *Z. Anorg. Allg. Chem.* **1973**, 399, 163.
- [16] M. Jansen, F. M. Chang, R. Hoppe, *Z. Anorg. Allg. Chem.* **1982**, 490, 101.
- [17] S. Pfeiffer, M. Jansen, *Z. Anorg. Allg. Chem.* **2007**, 633, 2558.
- [18] R. Hoppe, G. Brachtel, M. Jansen, *Z. Anorg. Allg. Chem.* **1975**, 417, 1.
- [19] E. Seipp, R. Hoppe, *Z. Anorg. Allg. Chem.* **1986**, 538, 123.
- [20] R. Hoppe, E. Seipp, *Z. Anorg. Allg. Chem.* **1985**, 522, 33.
- [21] R. Hoppe, E. Seipp, R. Baier, *J. Solid State Chem.* **1988**, 72, 52.
- [22] E. Seipp, R. Hoppe, *J. Less Common Met.* **1985**, 108, 279.
- [23] S. Pfeiffer, M. Jansen, *Z. Anorg. Allg. Chem.* **2009**, 635, 211.
- [24] M. M. Thackeray, W. I. F. David, P. G. Bruce, J. B. Goodenough, *Mat. Res. Bull.* **1983**, 18, 461.
- [25] A. Möller, P. Amann, V. Kataev, N. Schittner, *Z. Anorg. Allg. Chem.* **2004**, 630, 890.
- [26] G. Bauer, *Handbuch der Präparativen Anorganischen Chemie*, 3rd. ed., Vol. 1, F. Enke, Stuttgart 1975, p. 458.
- [27] Bruker Suite, version 2008/3, Bruker AXS Inc., Madison, USA, **2008**.
- [28] G. M. Sheldrick, SADABS — *Bruker AXS area detector scaling and absorption*, version 2008/1, University of Göttingen, Germany, **2008**.
- [29] G. M. Sheldrick, *Acta Crystallogr., Sect. A: Found. Crystallogr.* **2008**, 64, 112.
- [30] Further details may be obtained from Fachinformationszentrum Karlsruhe, 76344 Eggenstein-Leopoldshafen, Germany (fax: (+49)-7247-808-666; e-mail: crysdata(at)fiz-karlsruhe.de, [http://www.fiz-karlsruhe.de/request for deposited data.html](http://www.fiz-karlsruhe.de/request%20for%20deposited%20data.html)) on quoting the CSD number.
- [31] Graphical representations of the structures were made with ATOMS: E. Dowty, ATOMS — *a complete program for displaying atomic structures*, version 6.3.1, Shape Software, Kingsport, USA, **2006**.
- [32] S. Pfeiffer, D. Fischer, M. Jansen, *Z. Anorg. Allg. Chem.* **2008**, 634, 1673.
- [33] J. Nuss, S. Pfeiffer, S. van Smaalen, M. Jansen, *Acta Crystallogr., Sect. B: Struct. Sci.* **2009**, submitted.

Received: ((will be filled in by the editorial staff))  
Published online: ((will be filled in by the editorial staff))

**Table 1.** Crystallographic data for  $K_{29}Mn_{17}O_{34}$ ,  $Rb_{11}Mn_8O_{16}$ , and  $Cs_4Mn_3O_6$ .

Compound	$K_{29}Mn_{17}O_{34}$	$Rb_{11}Mn_8O_{16}$	$Cs_4Mn_3O_6$
Temperature /K		296(2)	
Formula weight	2611.75	1635.69	792.46
Crystal system		Orthorhombic	
Space group (no.)	<i>Ima2</i> (46)	<i>F222</i> (22)	<i>C222</i> (21)
Formula unit, <i>Z</i>	4	16	8
Lattice constants, <i>a, b, c</i> /Å	93.149(3), 10.0063(3), 6.0621(2)	12.2096(4), 20.1595(7), 43.712(2)	12.790(3), 21.123(4), 8.179(2)
Volume / Å <sup>3</sup>	5650.3(3)	10759.3(7)	2209.5(8)
$\rho_{calc}$ /g · cm <sup>3</sup>	3.070	4.039	4.765
Crystal shape, color		Needle, black	
Diffractometer	Smart APEX I, Bruker AXS		
X-ray radiaton, $\lambda$ / Å	0.71073		
$2\theta$ range /°	1.7 to 56.6	1.8 to 70.0	3.6 to 52.3
Index range, <i>h, k, l</i>	-118 - 120, -13 - 13, -8 - 8	-19 - 19, -31 - 32 -68 - 70	-15 - 15, -26 - 26, -10 - 10
Absorption correction	Multi-scan, <i>SADABS</i> [28]		
Reflection collected	25185	57764	9949
Data, $R_{int}$	6585, 0.032	11534, 0.055	2212, 0.051
No. of parameters	367	329	124
$R_1[F^2 > 2\sigma(F^2)]$	0.053	0.042	0.051
$wR(F^2)$	0.143	0.131	0.122
$\Delta\rho_{max}, \Delta\rho_{min}$ /e · Å <sup>3</sup>	1.08, -1.04	1.88, -3.13	1.72, -1.80
CSD no. [30]	420663	420662	420664

**Table 2.** Atomic coordinates and equivalent isotropic displacement parameters  $U_{\text{eq}}/10^4 \text{ \AA}^2$  for  $\text{K}_{29}\text{Mn}_{17}\text{O}_{34}$  (standard deviations).

Atom	Site	<i>x</i>	<i>y</i>	<i>z</i>	$U_{\text{eq}}$
K1	8 <i>c</i>	0.0436(1)	0.3384(1)	0.1203(3)	294(3)
K2	8 <i>c</i>	0.1301(1)	0.6590(2)	0.0899(3)	426(5)
K3	8 <i>c</i>	0.2161(1)	0.3401(2)	0.0466(3)	608(6)
K4	8 <i>c</i>	0.1980(1)	0.6639(2)	0.0360(3)	552(5)
K5	8 <i>c</i>	0.1122(1)	0.3367(2)	0.0475(3)	514(5)
K6	8 <i>c</i>	0.1822(1)	0.1631(2)	0.3956(4)	581(6)
K7	8 <i>c</i>	0.0955(1)	0.6659(2)	0.9047(3)	457(5)
K8	8 <i>c</i>	0.2327(1)	0.6626(3)	0.9207(4)	710(7)
K9	8 <i>c</i>	0.0253(1)	0.6614(2)	0.0516(3)	548(6)
K10	8 <i>c</i>	0.0092(1)	0.3371(2)	0.9107(3)	455(5)
K11	8 <i>c</i>	0.1476(1)	0.3392(2)	0.9733(4)	576(5)
K12	8 <i>c</i>	0.0607(1)	0.8411(2)	0.5097(3)	483(5)
K13	8 <i>c</i>	0.0771(1)	0.3404(2)	-0.1163(3)	425(4)
K14	8 <i>c</i>	0.1637(1)	0.6599(2)	-0.1505(3)	431(5)
K15	4 <i>b</i>	¼	0.3392(3)	0.8300(5)	458(7)
Mn1	8 <i>c</i>	0.0293(1)	0.5100(1)	0.5303(2)	162(2)
Mn2	8 <i>c</i>	0.1765(1)	0.4927(1)	0.4218(2)	251(3)
Mn3	8 <i>c</i>	0.2058(1)	0.5014(1)	0.4968(2)	295(3)
Mn4	8 <i>c</i>	0.1174(1)	0.4940(1)	0.5208(2)	211(2)
Mn5	8 <i>c</i>	0.1469(1)	0.4868(1)	0.4664(2)	270(2)
Mn6	8 <i>c</i>	0.0590(1)	0.5126(1)	0.5060(2)	212(2)
Mn7	4 <i>a</i>	0	½	0.4567(2)	143(3)
Mn8	8 <i>c</i>	0.2353(1)	0.5118(1)	0.4304(2)	346(3)
Mn9	8 <i>c</i>	0.0883(1)	0.5031(1)	0.4425(2)	172(2)
O1	8 <i>c</i>	0.1885(1)	0.5917(5)	0.6493(8)	319(12)
O2	8 <i>c</i>	0.1010(1)	0.4001(5)	0.6694(8)	338(12)
O3	8 <i>c</i>	0.0173(1)	0.4158(5)	0.3094(8)	281(11)
O4	8 <i>c</i>	0.1050(1)	0.5910(5)	0.3008(9)	349(13)
O5	8 <i>c</i>	0.2234(1)	0.4081(7)	0.639(1)	557(17)
O6	8 <i>c</i>	0.0708(1)	0.4127(6)	0.299(1)	438(14)
O7	8 <i>c</i>	0.0450(1)	0.4333(6)	0.715(1)	494(14)
O8	8 <i>c</i>	0.1929(1)	0.3983(6)	0.291(1)	550(17)
O9	8 <i>c</i>	0.0440(1)	0.6172(5)	0.370(1)	425(13)
O10	8 <i>c</i>	0.0133(1)	0.5954(5)	0.681(1)	272(11)
O11	8 <i>c</i>	0.1349(1)	0.5763(6)	0.677(1)	518(16)
O12	8 <i>c</i>	0.1592(1)	0.5845(6)	0.277(1)	553(16)
O13	4 <i>b</i>	¼	0.6076(9)	0.598(2)	537(21)
O14	8 <i>c</i>	0.1624(1)	0.4012(6)	0.625(1)	486(16)
O15	4 <i>b</i>	¼	0.427(1)	0.256(2)	981(30)
O16	8 <i>c</i>	0.0745(1)	0.6073(6)	0.652(1)	441(14)
O17	8 <i>c</i>	0.1317(1)	0.3772(6)	0.359(1)	489(15)
O18	8 <i>c</i>	0.2192(1)	0.6175(7)	0.320(1)	630(18)

**Table 3.** Atomic coordinates and equivalent isotropic displacement parameters  $U_{\text{eq}}/10^4 \text{ \AA}^2$  for  $\text{Rb}_{11}\text{Mn}_8\text{O}_{16}$  (standard deviations).

Atom	Site	<i>x</i>	<i>y</i>	<i>z</i>	$U_{\text{eq}}$
Rb1	8 <i>f</i>	0	0.6767(1)	0	570(8)
Rb2	8 <i>i</i>	¼	0.5927(1)	¼	294(5)
Rb3	16 <i>k</i>	−0.0051(2)	0.6610(1)	0.2715(1)	242(3)
Rb4	16 <i>k</i>	0.2452(2)	0.9089(1)	0.0694(1)	257(4)
Rb5	16 <i>k</i>	−0.2426(2)	0.9130(1)	0.1132(1)	245(4)
Rb6	16 <i>k</i>	0.0059(2)	0.1651(1)	0.0445(1)	281(4)
Rb7	16 <i>k</i>	−0.2573(2)	0.9169(1)	0.2019(1)	271(4)
Rb8	16 <i>k</i>	−0.5050(2)	0.6692(1)	0.1406(1)	293(4)
Rb9	16 <i>k</i>	0.0037(2)	0.6741(1)	0.1769(1)	335(4)
Rb10	16 <i>k</i>	−0.2556(2)	0.9215(1)	0.0180(1)	276(4)
Rb11	16 <i>k</i>	0.4977(1)	0.1575(1)	0.0901(1)	281(3)
Rb12	16 <i>k</i>	0.2470(2)	0.5746(1)	0.1619(1)	493(5)
Mn1	4 <i>a</i>	0	0	0	129(9)
Mn2	4 <i>b</i>	0	0	½	181(10)
Mn3	8 <i>g</i>	0	0	0.1877(1)	125(6)
Mn4	8 <i>g</i>	0	0	0.6254(1)	135(7)
Mn5	8 <i>g</i>	0	0	0.0636(1)	160(7)
Mn6	8 <i>g</i>	0	0	0.2519(1)	167(6)
Mn7	8 <i>g</i>	0	0	0.1244(1)	154(7)
Mn8	8 <i>g</i>	0	0	0.5613(1)	136(6)
Mn9	8 <i>g</i>	0	0	0.3124(1)	190(7)
Mn10	8 <i>h</i>	¼	¼	−0.0953(1)	170(7)
Mn11	8 <i>h</i>	¼	¼	0.0925(1)	186(7)
Mn12	8 <i>h</i>	¼	¼	0.1560(1)	163(7)
Mn13	8 <i>h</i>	¼	¼	−0.0317(1)	146(6)
Mn14	8 <i>h</i>	¼	¼	0.2190(1)	173(7)
Mn15	8 <i>h</i>	¼	¼	0.7816(1)	138(7)
Mn16	8 <i>h</i>	¼	¼	0.0308(1)	157(7)
Mn17	8 <i>h</i>	¼	¼	0.8436(1)	142(6)
O1	8 <i>i</i>	¼	0.1808(8)	¼	501(46)
O2	8 <i>j</i>	0.643(1)	¼	¼	273(35)
O3	16 <i>k</i>	0.3978(7)	0.9953(7)	0.0935(1)	230(21)
O4	16 <i>k</i>	0.6580(8)	0.2889(5)	0.0016(2)	276(23)
O5	16 <i>k</i>	−0.0964(9)	0.9669(6)	0.1586(2)	320(27)
O6	16 <i>k</i>	0.8573(9)	0.2601(7)	0.0630(2)	329(29)
O7	16 <i>k</i>	0.4101(9)	0.0420(6)	0.1537(2)	261(24)
O8	16 <i>k</i>	0.8320(9)	0.2020(6)	0.1901(2)	271(24)
O9	16 <i>k</i>	−0.3502(9)	0.7195(6)	0.1858(2)	270(26)
O10	16 <i>k</i>	−0.0983(9)	0.0239(6)	0.0305(2)	334(30)
O11	16 <i>k</i>	0.1023(8)	0.9866(6)	0.2191(2)	275(28)
O12	16 <i>k</i>	0.574(1)	0.0538(6)	0.0324(2)	367(32)
O13	16 <i>k</i>	−0.3550(9)	0.7697(7)	0.1257(2)	363(28)
O14	16 <i>k</i>	0.813(1)	0.3093(6)	0.1241(2)	353(28)
O15	16 <i>k</i>	−0.016(1)	0.0687(5)	0.0938(2)	484(39)
O16	16 <i>k</i>	−0.283(1)	0.8183(6)	0.0627(2)	551(37)
O17	16 <i>k</i>	0.047(1)	0.9362(6)	0.2807(2)	449(38)

**Table 4.** Atomic coordinates and equivalent isotropic displacement parameters  $U_{\text{eq}}/10^4 \text{ \AA}^2$  for  $\text{Cs}_4\text{Mn}_3\text{O}_6$  (standard deviations).

Atom	Site	<i>x</i>	<i>y</i>	<i>z</i>	$U_{\text{eq}}$
Cs1	4 <i>g</i>	0	0.3431(1)	0	373(6)
Cs2	4 <i>h</i>	0	0.3266(2)	½	532(8)
Cs3	8 <i>l</i>	0.2573(2)	0.4108(1)	0.1176(2)	479(6)
Cs4	8 <i>l</i>	0.2425(3)	0.4230(1)	−0.3960(2)	505(6)
Cs5	8 <i>l</i>	−0.0078(2)	0.1689(1)	0.2515(2)	359(4)
Mn1	4 <i>j</i>	0	½	−0.1741(6)	277(13)
Mn2	2 <i>c</i>	½	0	½	294(20)
Mn3	4 <i>k</i>	¼	¼	−0.0206(6)	311(12)
Mn4	4 <i>k</i>	¼	¼	0.3102(6)	305(14)
Mn5	4 <i>k</i>	¼	¼	−0.3524(5)	320(16)
Mn6	2 <i>d</i>	0	0	½	330(20)
Mn7	4 <i>i</i>	0	0	0.1647(9)	451(16)
O1	4 <i>e</i>	0.600(2)	0	0	286(55)
O2	8 <i>l</i>	−0.073(2)	0.4493(9)	−0.325(2)	359(45)
O3	8 <i>l</i>	0.151(2)	0.259(1)	0.151(2)	611(66)
O4	8 <i>l</i>	0.161(1)	0.214(1)	0.469(2)	446(56)
O5	8 <i>l</i>	0.197(2)	0.305(1)	−0.174(2)	708(87)
O6	8 <i>l</i>	0.596(2)	0.527(1)	0.332(3)	606(68)
O7 <sup>[a]</sup>	8 <i>l</i>	0.529(2)	0.565(1)	−0.002(4)	326(69)

[a] O7 is located on a split position with site occupation factor (s.o.f) fixed to 0.5.

**Table 5.** Mn—O interatomic distances /Å for  $K_{29}Mn_{17}O_{34}$ ,  $Rb_{11}Mn_8O_{16}$ , and  $Cs_4Mn_3O_6$  (standard deviations).

<b><math>K_{29}Mn_{17}O_{34}</math></b>				<b><math>Rb_{11}Mn_8O_{16}</math></b>				<b><math>Cs_4Mn_3O_6</math></b>						
Mn1	-O3	1.981(5)	Mn5	-O12	1.893(7)	Mn1	-O10	1.858(9) ×4	Mn10	-O6	1.93(1) ×2	Mn1	-O1	1.91(2) ×2
	-O7	1.994(6)		-O14	1.932(6)	Mn2	-O12	2.00(1) ×4		-O14	1.901(9) ×2		-O2	1.89(2) ×2
	-O9	1.990(5)		-O17	1.904(6)	Mn3	-O5	1.86(1) ×2	Mn11	-O13	1.98(1) ×2	Mn2	-O2	2.02(2) ×4
	-O10	1.948(4)	Mn6	-O6	1.948(6)		-O11	1.874(9) ×2		-O16	1.94(1) ×2	Mn3	-O3	1.90(2) ×2
Mn2	-O1	2.036(5)		-O7	1.990(6)	Mn4	-O3	1.877(8) ×2	Mn12	-O9	1.889(9) ×2		-O5	1.85(2) ×2
	-O8	1.966(6)		-O9	1.932(5)		-O7	1.857(9) ×2		-O13	1.885(9) ×2	Mn4	-O3	1.83(2) ×2
	-O12	2.052(6)		-O16	1.936(5)	Mn5	-O10	1.94(1) ×2	Mn13	-O4	1.898(9) ×2		-O4	1.89(2) ×2
	-O14	2.020(6)	Mn7	-O3	2.029(4) ×2		-O15	1.923(8) ×2		-O6	1.908(9) ×2	Mn5	-O4	2.00(2) ×2
Mn3	-O1	2.064(5)		-O10	2.078(4) ×2	Mn6	-O11	1.921(9) ×2	Mn14	-O1	1.94(1) ×2		-O5	1.98(2) ×2
	-O5	2.074(6)	Mn8	-O5	1.976(7)		-O17	1.89(1) ×2		-O9	2.00(1) ×2	Mn6	-O6	1.93(2) ×4
	-O8	2.019(6)		-O13	1.959(7)	Mn7	-O5	2.01(1) ×2	Mn15	-O2	1.91(1) ×2	Mn7	-O6	1.92(3) ×2
	-O18	2.013(7)		-O15	1.931(9)		-O15	1.935(9) ×2		-O8	1.86(1) ×2		-O7 <sup>[a]</sup>	1.94(3) ×2
Mn4	-O2	2.010(5)		-O18	1.954(7)	Mn8	-O3	1.882(8) ×2	Mn16	-O4	1.971(9) ×2		-O7 <sup>[a]</sup>	1.97(3) ×2
	-O4	2.013(5)	Mn9	-O2	2.087(5)		-O12	1.89(1) ×2		-O16	2.00(1) ×2			
	-O11	2.057(6)		-O4	1.988(5)	Mn9	-O7	2.029(9) ×2	Mn17	-O8	2.024(9) ×2			
	-O17	2.024(6)		-O6	2.056(5)		-O17	1.975(9) ×2		-O14	2.004(9) ×2			
Mn5	-O11	1.917(6)		-O16	2.086(5)									

[a] O7 is located on a split position.

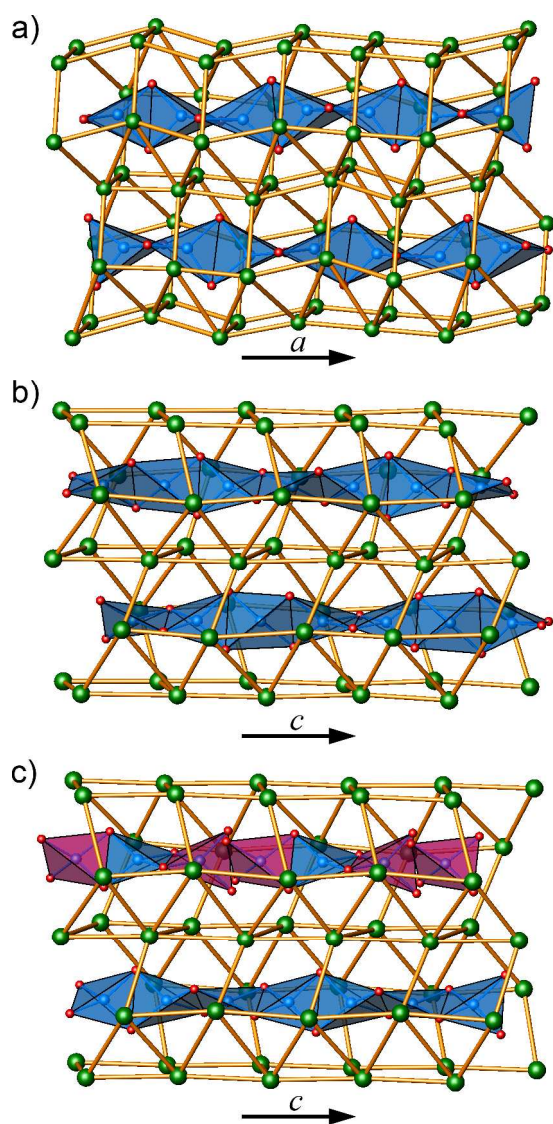
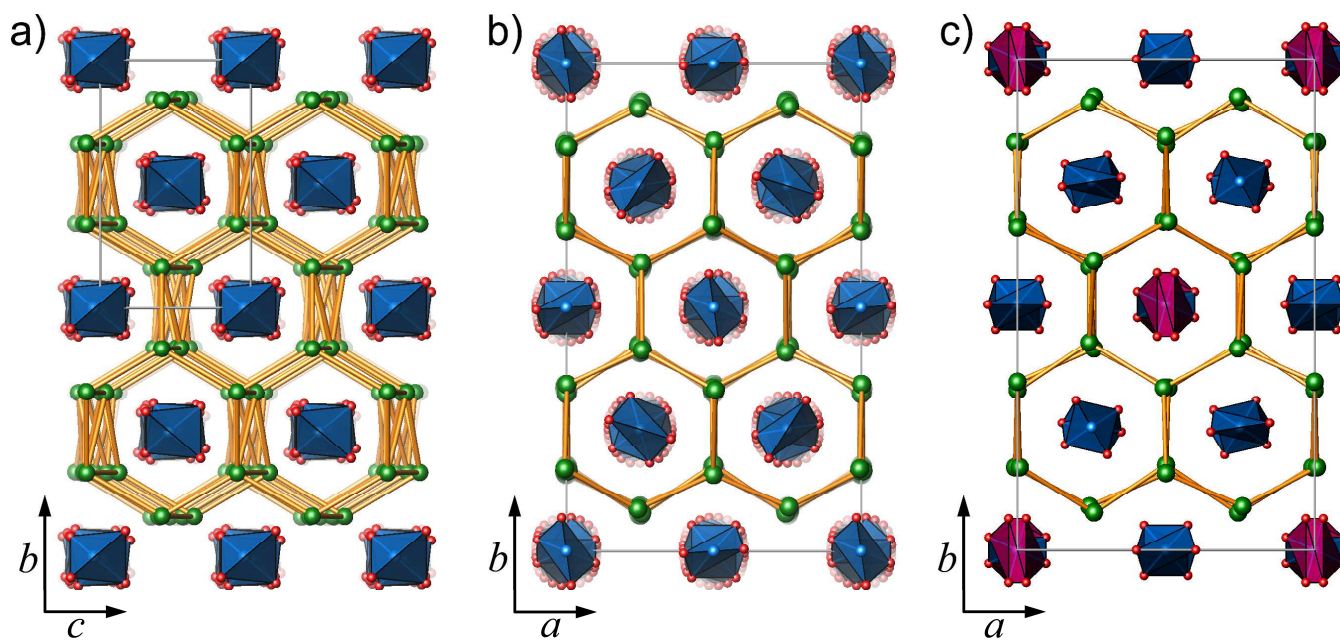


**Figure 1.** Fragments of the crystal structures of a)  $K_{29}Mn_{17}O_{34}$ , b)  $Rb_{11}Mn_8O_{16}$ , and c)  $Cs_4Mn_3O_6$ . Colour code: alkali metals (green),  $MnO_4$  tetrahedra (blue), disordered  $MnO_4$  tetrahedra due to splitting of O-atoms (pink), oxygen atoms (red), shortest distances between alkali metals (orange) [31].



!!Please print figure 2 in 2-column format!!

**Figure 2.** Projection of the crystal structures of a)  $\text{K}_{29}\text{Mn}_{17}\text{O}_{34}$ , b)  $\text{Rb}_{11}\text{Mn}_8\text{O}_{16}$ , and c)  $\text{Cs}_4\text{Mn}_3\text{O}_6$ . View along  $[1\ 0\ 0]$  (a) and  $[0\ 0\ 1]$  (b, c) direction, with margins of the unit cells (grey). Same colour code as in Fig. 1 [31].

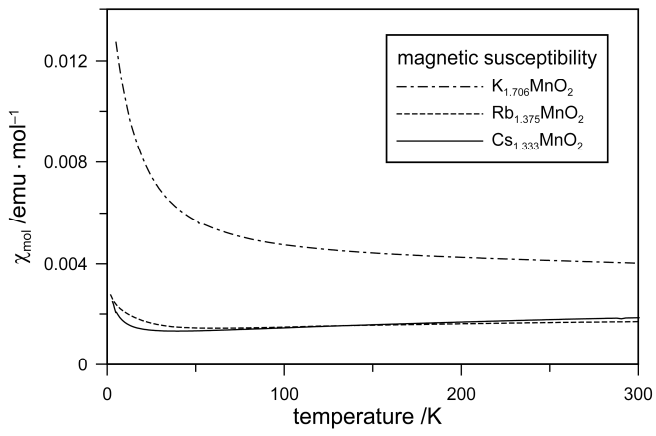
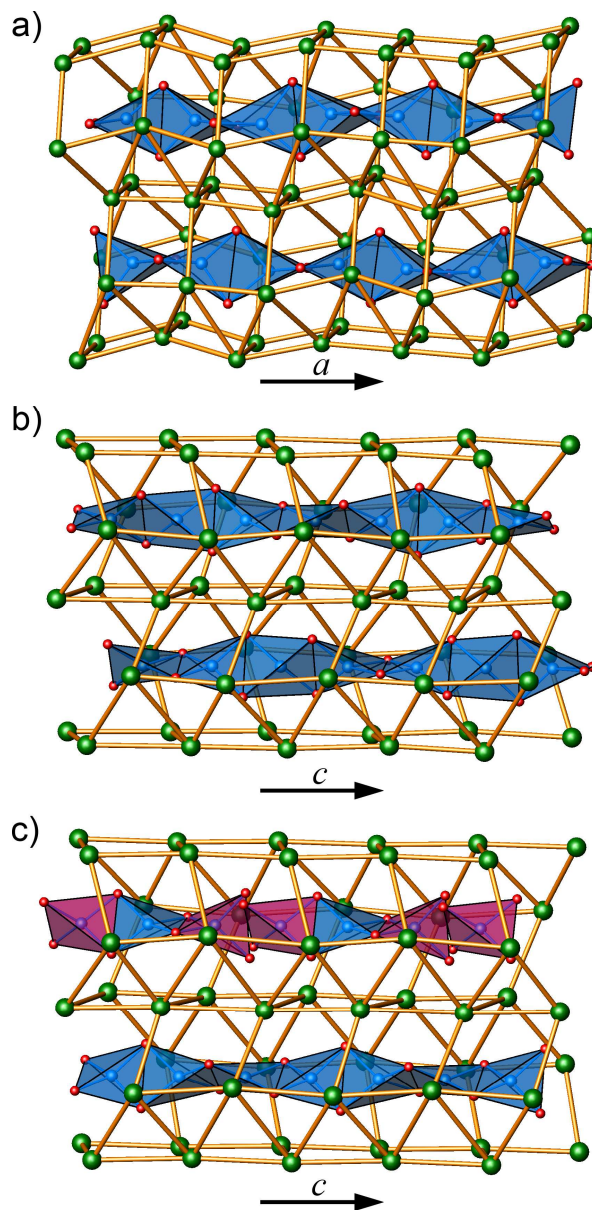
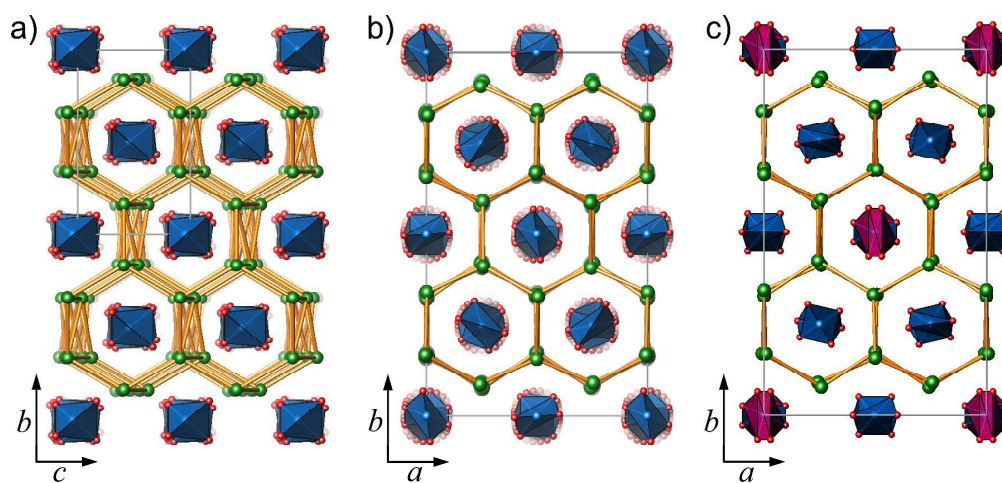


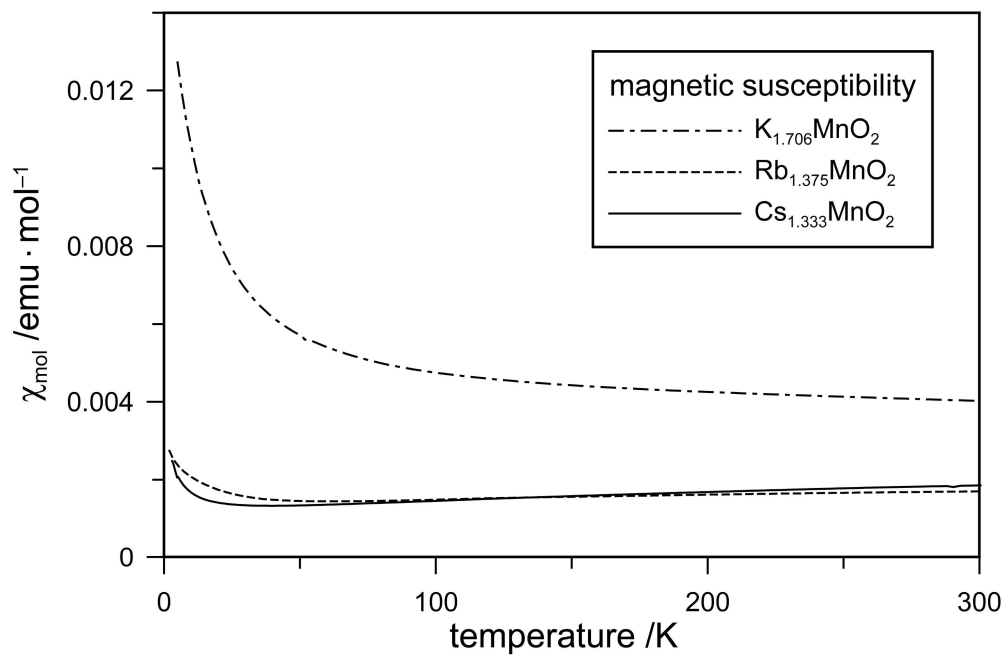
**Figure 3.** Molar magnetic susceptibilities versus temperature, normalized to one manganese atom per formula unit.



Fragments of the crystal structures of a)  $\text{K}_{29}\text{Mn}_{17}\text{O}_{34}$ , b)  $\text{Rb}_{11}\text{Mn}_8\text{O}_{16}$ , and c)  $\text{Cs}_4\text{Mn}_3\text{O}_6$ . Colour code: alkali metals (green),  $\text{MnO}_4$  tetrahedra (blue), disordered  $\text{MnO}_4$  tetrahedra due to splitting of O-atoms (pink), oxygen atoms (red), shortest distances between alkali metals (orange) [31].  
71x146mm (600 x 600 DPI)



Projection of the crystal structures of a)  $\text{K}_{29}\text{Mn}_{17}\text{O}_{34}$ , b)  $\text{Rb}_{11}\text{Mn}_8\text{O}_{16}$ , and c)  $\text{Cs}_4\text{Mn}_3\text{O}_6$ . View along  $[1\ 0\ 0]$  (a) and  $[0\ 0\ 1]$  (b, c) direction, with margins of the unit cells (grey). Same colour code as in Fig. 1 [31].  
227x106mm (600 x 600 DPI)



Molar magnetic susceptibilities versus temperature, normalized to one manganese atom per formula unit.  
130x84mm (600 x 600 DPI)